**Proteomic study of neuron and astrocyte cultures from senescence-accelerated mouse SAMP8 reveals degenerative changes**

*Cristina Díez-Vives[1], Marina Gay[2], Silvia García-Matas[1], Francesc Comellas[3], Montserrat Carrascal[2], Joaquín Abian[2], Arantxa Ortega[4], Rosa Cristòfol[1], Coral Sanfeliu[1]*

[1]Department of Brain Ischemia and Neurodegeneration, Institut d'Investigacions Biomèdiques de Barcelona (IIBB), CSIC-IDIBAPS, Barcelona, Spain.
[2]CSIC-UAB Proteomics Laboratory Facilities, Barcelona, Spain.
[3]Department of Applied Mathematics IV, Universitat Politècnica de Catalunya (UPC), Barcelona, Spain.
[4]Department of Pathology, University Hospital Vall d'Hebron (HUVH), Barcelona, Spain.

Corresponding author:
Coral Sanfeliu, PhD
Department of Brain Ischemia and Neurodegeneration
Institut d'Investigacions Biomèdiques de Barcelona (IIBB)
CSIC-IDIBAPS
Rosselló 161, 6th floor, 08036 Barcelona, Spain.
E-mail: coral.sanfeliu@iibb.csic.es
Phone: (+34) 933638338
Fax: (+34) 933638301

**Abbreviations: AD**, Alzheimer's disease; **Aldh2**, aldehyde dehydrogenase mitochondrial; **CHAPS**, 3-[(3-cholamidopropyl) dimethylammonio] propanesulfonate; **Cox**, cytochrome oxidase; **DMEM**, Dulbecco's Modified Eagle's Medium**; FBS**, fetal bovine serum; **HPI**, human protein interactome network; **MALDI-TOF-MS**, matrix-assisted laser desorption/ionization-time of flight-mass spectrometry; **MOWSE**, molecular weight search; **PBS**, phosphate buffered saline; **PMF**, peptide mass fingerprint; **PP1**, serine/threonine-protein phosphatase type 1; **Ppp1ca**, Serine/threonine-protein phosphatase PP1-alpha catalytic subunit; **SAMP8**, senescence-accelerated prone mouse strain 8; **SAMR1**, senescence-accelerated resistant mouse strain 1; **SDS-PAGE**, sodium dodecyl sulfate-polyacrylamide gel electrophoresis; **SUMO**, small ubiquitin-like modifier.

**Abstract**

Senescence-accelerated prone (SAMP) strain 8 mice suffer an earlier development of cognitive age-related pathologies and a shorter life span than conventional mice. Protein alterations in astrocytes, in addition to those in neurons, may contribute to neurodegenerative damage. We applied proteomics techniques to study cell-specific early markers of brain aging-related degeneration in SAMP8. The two-dimensional protein expression patterns of the SAMP8 neuron and astrocyte cultures were compared to those obtained from senescence-resistant strain 1 (SAMR1) cultures. Differentially expressed spots were identified by matrix-assisted laser desorption/ionization-time of flight peptide map fingerprinting and database search. Proteins belonged to cell pathways of energy metabolism, biosynthesis, cell transduction and signaling, stress response and the maintenance of cytoskeletal functions. Most of the changes were cell type specific. However, there was a general increase in cell transduction, signaling and stress-related proteins and a decrease in cytoskeletal proteins. In addition, neurons showed an increased expression of proteins involved in biosynthetic pathways. A number of the protein alterations have been previously reported in the brain tissue proteome of SAMP8, aged brain or AD brain. Alterations in neuron and astrocyte proteoma indicated that both cell types are involved in the brain degenerative changes of SAMP8 mice. However, network analysis suggests that neuronal changes are more complex and have a greater influence.

**Keywords:**

Alzheimer's disease, brain aging, differential proteomics, neuron and astrocyte cultures, SAMP8 mouse

**Running title:**

Proteomics of SAMP8 neurons and astrocytes

## Introduction

Age-associated neurodegeneration is the subject of intense research, in the hope of decreasing the incidence of mentally disabling diseases in the elder population. Alzheimer's disease (AD) is the most common age-related neurodegenerative disease with an estimated 26 million people living with the condition worldwide. This number will quadruplicate by 2050.

The senescence-accelerated prone mouse strain 8 (SAMP8) is an established animal model for studying age-related cognitive decline, including the contribution of amyloid beta neuropathology (Flood and Morley, 1998; Butterfield and Poon 2005; Pallas *et al.* 2008; Tomobe and Nomura 2009). SAMP8 was obtained through phenotypic selection from a common genetic pool of AKR/J mice. It has a shorter life span than the reference strain (senescence-accelerated resistant mouse strain 1 [SAMR1]) and suffers age-related cognitive impairment (Takeda, 1999, 2009). Brain studies of SAMP8 have shown elevated levels of amyloid beta (Morley *et al.* 2002) with plaque-like formation (Takemura *et al*. 1993), tauopathy alterations (Canudas *et al.* 2005) and oxidative stress (Butterfield *et al.* 1997; Farr *et al.* 2003; Sureda *et al*. 2006), mainly attributed to mitochondrial dysfunction (Fujibayashi *et al*. 1998). Several authors have undertaken proteomic studies of SAMP8 brain tissue in a search for abnormal expression or oxidation of proteins that could shed light on the pathologically altered pathways (Butterfield and Poon 2005; Nabeshi *et al.* 2005; Wang *et al.* 2008). Although significant insights have been obtained, the complete protein alterations underlying SAMP8 brain changes are far from been elucidated. Moreover, it is not known the differential involvement of the main brain cell types, neurons and astrocytes. We and others recently demonstrated that SAMP8 cultured astrocytes exhibited age-related disturbances (García-Matas *et al.* 2008; Lü *et al.* 2008, 2009) and reduced neuroprotective capacity (García-Matas *et al.* 2008), as compared to SAMR1 astrocytes. Studies on SAMP8 cultured neurons confirmed some age-related disturbances, such as reduced mitochondrial functionality and higher vulnerability to oxidative injuries (unpublished results). In this work, we used the powerful proteomic technology to analyze SAMP8 brain protein expression changes down to the cellular level, in order to dissect the neuron and astrocyte contribution to pathological aging of the brain. For this purpose, we used cultures of cerebral cortical neurons and astrocytes of SAMP8 and SAMR1 mouse and analyzed the differential changes that appeared in the neuronal and astrocytic proteoma of SAMP8, as compared to SAMR1.

## Materials and methods

### Animals and reagents

SAMR1 and SAMP8 mouse breeders were purchased from Charles River Laboratories (Lyon, France) and their colonies were established in the University of Barcelona's Animal House. Animals were maintained and handled in compliance with protocols approved by the Generalitat (Autonomous Government of Catalonia), Spain, in accordance with EU guidelines, and in compliance with the Office of Laboratory Animal Welfare/National Institute of Health (identification number A5224-01).

Culture chemicals were purchased from Sigma-Aldrich Co (St. Louis, MO, USA) if not otherwise stated. Reagents and analytical grade chemicals for electrophoresis and gel staining were obtained from Merck (Darmstadt, Germany) or as indicated below.

### Cell cultures

*Neuron cultures*

Primary cultures of neurons were prepared from the fetal cerebral cortices of E15-E16 SAMR1 and SAMP8 mice, as previously described (Frandsen and Schousboe, 1990). Neocortices were dissected and mechanically minced. Tissue was then dissociated to single cells by mild trypsinization (0.02% w/v) at 37°C for 10 min followed by trituration in a DNAse solution (0.004% w/v) containing a soybean trypsin inhibitor (0.05% w/v). The cells were re-suspended in a Dulbecco's Modified Eagle's Medium (DMEM; Biochrom AG, Berlin, Germany) supplemented with 100 mU/L insulin, 7 μM p-aminobenzoic acid, 0.2 mM glutamine, 100 μg/mL gentamicin and 10% fetal bovine serum (FBS; Gibco-Invitrogen, Paisley, UK). The cell suspension was seeded at 32 x $10^4$ cell/$cm^2$ in T75 flasks (Nunc, Roskilde, Denmark) that had been precoated with poly-D-lysine, and incubated for 7-8 days in a humidified 5% $CO_2$/95% air atmosphere at 37ºC. A mixture of 5 μM 5-fluoro-2′-deoxyuridine and 20 μM uridine was added after 48 h in culture to prevent glial proliferation without damaging neurons. Highly pure neuron cultures were obtained, with glial cell contamination below 5-10%. Neurons were collected after 7 days in vitro.

*Astrocyte cultures*

Primary cultures of astrocytes were established from cerebral cortical tissue of 2-day old SAMR1 and SAMP8, as previously described (García-Matas *et al.* 2008) Briefly, cortices were dissected free of the meninges, diced into small cubes and dissociated by incubation with a 0.25 % trypsin / 1 mM EDTA solution (Gibco) for 25 min. After a further mechanical disaggregation, cells were resuspended in DMEM supplemented with 2.5 mM glutamine, 100 μg/mL gentamycin and 20% FBS. Cells were seeded at 5 x $10^4$ cell/$cm^2$ in T75 flasks and incubated at 37ºC in a humidified atmosphere of 5% $CO_2$ -95% air. The culture medium was changed twice a week. The concentration of FBS was changed to 15% and 10% after one and two weeks of culture, respectively. After 3 weeks, the flasks were shaken in an orbital shaker at 200 rpm for 4 h to dislodge microglia and the attached astrocyte monolayer was collected. This purified fraction contained more than 90-95% astrocytes, with a minor fraction of contaminating microglia.

**Two-dimensional gel electrophoresis**

*Sample preparation*

The neuron or astrocyte monolayer of a culture flask was washed with cold phosphate buffered saline (PBS) and maintained on ice while the cells were scraped with a rubber policeman. Cells were collected aseptically, centrifuged at 400 x g and rinsed with PBS. Three different flasks from each of two independent cultures of SAMR1 and SAMP8 astrocytes were harvested for the study. For neurons, also triplicate flasks were harvested from each of three independent cultures of SAMR1 and SAMP8. See the outline of the experimental design and main results in the flow chart (Fig. 1). The pellets were stored at -80ºC until processed. Frozen samples were resuspended in 500μl of cold lysis buffer (7 M urea, 2 M thiourea, 4 % 3-[(3-cholamidopropyl) dimethylammonio] propanesulfonate (CHAPS), 40 mM Tris-base, 10 mM dithiothreitol and 1 mM phenyl-methylsulfonyl fluoride, sonicated for 30 s, shaken orbitally for 10 min, sonicated again for 30 s and centrifuged at 15000 ×g for 10 min, all at 4ºC. Proteins were precipitated from the supernatant by orbital shacking in 10 % trichloroacetic acid for 90 min at 4ºC and centrifugation at 15000 ×g for 10 min (Quero *et al.* 2004). The protein extracts were rinsed with iced acetone, resuspended in 500μl of rehydration buffer (7 M urea, 2 M thiourea, 2% CHAPS, 97mM DeStreak, 0.5 % IPG Buffer), and stored in aliquots at -80ºC. Protein concentration was determined using the RC DC Protein Assay kit (Bio-Rad, Hercules, CA, USA), according to the manufacturer's instructions.

*Isoelectric focusing*

First dimension isoelectrofocusing was performed on IPG strips (pH 3-10, 18 and 24 cm for astrocytes and neurons, respectively) using an IPGphor unit (GE Healthcare, Uppsala, Sweden). A sample containing 100 µg of proteins was diluted with rehydration buffer to a volume 350 - 450 µL (Quero *et al.* 2004), loaded on strips, and then rehydrated without voltage application for 6 h and at 50 V for 6 h. Electrophoresis was performed at 20ºC under the following conditions: 500 V (gradient over 1h), 1,000 V (gradient 1h), 4,000 V (gradient 1h), 8,000 V (gradient 1h) and 8,000 V (fixed to 60,000 1h). The electrofocused strips were stored at -80ºC until sodium dodecyl sulfate polyacrylamide gel electrophoresis (SDS-PAGE).

*SDS-PAGE*

The strips were immersed for 15 min in equilibration solution (50 mM Tris, 6 M urea, 30% glycerol, 2% SDS) containing 1% dithiothreitol and then transferred to another equilibration solution containing 2.5% iodoacetamide and shaken for 15 min. The separation of proteins was carried out using self-cast 8% and 12% acrylamide gels in an Ettan Dalt Six electrophoresis system (GE Healthcare) at 2.5 W per gel for 30 min followed by 17 W/gel for the next 5h. Six different neuron samples, including one triplicate flask from each of the three SAMR1 and three SAMP8 cultures of the study, were simultaneously run. The procedure was repeated twice with the two remaining triplicate flasks. Next, astrocyte samples were processed similarly, also running one of the triplicate culture flaks at a time. Protein spots in the 30 gels generated were visualized by silver staining according to the procedure outline elsewhere (Shevchenko *et al.* 1996).

**Image analysis and statistics**

The gels were washed with water, scanned using a densitometer (GS-800, Bio-Rad) and analyzed with ImageMaster™ Platinum 5.0 software (GE Healthcare). A total of nine gels for each cell type and mouse strain were analyzed. Neuron and astrocyte gels were analyzed separately. A reference gel was constructed for each cell type using as a basis the gel with the maximum number of distinct spots. All the spots for a given gel were matched to the corresponding reference gel by means of the automatic analyses. They were then verified manually by local pattern comparison. The quantification of proteins was expressed as the relative volumes of all spots in each gel (% volume). Analytical and

biological coefficients of variance in these assays were typically up to 30% and 50%, respectively (Ramirez-Boo et al., 2006). Therefore, protein spots of SAMP8 mice were accepted as different from SAMR1 mice when the protein content was increased or decreased by at least two fold, and the Student's *t*-test confirmed the statistical significance of the results ($p < 0.05$). Analysis was re-evaluated by visual inspection.

**Protein identification**

The spots of interest were excised and subjected to in-gel digestion with trypsin as described elsewhere (Shevchenko *et al.* 1996). Tryptic peptides were extracted from the gel with acetonitrile/water/trifluoroacetic acid, and extracts were evaporated to dryness and redissolved in acetonitrile/water (1/1), 1% acetic acid. Peptide mass fingerprint (PMF) identification (was performed by matrix-assisted laser desorption-time of flight-mass spectrometry (MALDI-TOF-MS) in a Voyager DE PRO (Applied Biosystems, Barcelona) working in positive refrectron mode. A 0.5 µL sample fraction was loaded in a 96 x 2 well plate, was mixed with 0.5 µL of matrix (3 mg/mL α-ciano-4-hidroxycinamic acid in acetonitrile/water 2/1 0.1% trifluoroacetic acid) and was let to dry. Spectra were externally calibrated using a standard mixture (des-Arg1-bradiquinine (Mr 904.46), Glu1-fibrinopeptid B (Mr 2465.2), corticotropin-inhibiting peptide (Mr 3657.93) and, when possible, an internal calibration using the ions derived from the trypsin autodigestion was used. The Protein Prospector (http://donatello.ucsf.edu) and MASCOT (Matrix Science, Inc, Boston, MA) software packages were used for data mining in the Swiss-Prot (European Bioinformatics Institute, Heidelberg, Germany) and National Center for Biotechnology Information (Bethesda, MD) databases. The following parameters were used: peptide mass tolerance 100 ppm, enzyme set as trypsin and allowance up to two missed cleavages, static modification was cysteine carbamidomethylated (+57 Da) and dynamic modification was methionine oxidation.

**Network analysis**

A network analysis was performed with the Combinatorica and Graph Utilities packages of Mathematica, version 6 (Wolfram Research, Inc., Champaign, IL), and the Python graph package NetworkX, version 0.36 (Los Alamos National Laboratory, NM) for both neuronal and astrocytic differential proteins. The constructed networks mathematicaly modeled the interactions between the whole set of differentially expressed proteins in neurons and in astrocytes. Nodes indicate the proteins and edges indicate their interactions. Complexity of

the node interactions correlates with the functional complexity of the proteins involved. Protein-protein interactions were obtained from the Human Protein Reference Database (http://www.hprd.org) (Mishra et al. 2006). The Human Protein Interactome network (HPI) was build with 35,021 interactions between 9,462 proteins, and its largest connected component has 34,876 interactions between 9,047 proteins. Human genes homologous to the differentially expressed mouse genes were obtained from the Entrez Gene database (NCBI, NIH). The following parameters were analyzed: a) *Average distance*, distance between the protein nodes that indicates the number of intermediate links through the shortest path; b) *Closeness centrality*, reciprocal of the mean shortest distance between a node and all HPI connected nodes that is a measure of the speed of the communication from each node protein to other reachable nodes in the whole HPI network; c) *Degree of centrality*, number of HPI links incident upon a node; d) *Betweenness centrality*, fraction of the shortest pathways between all HPI node pars that go through a given node; and e) *Clustering coefficient*, ratio of existing interconnections among all neighbors of a given node and their maximal possible interconnections.

**Western blotting**

One representative protein for each cell type was selected to validate the proteomics results by Western blotting. Selected proteins were PP1-alpha catalytic subunit (Ppp1ca) for neurons and aldehyde dehydrogenase (Aldh2) for astrocytes. Two different membranes, each loaded with four samples of SAMR1 and four samples of SAMP8 were analyzed for each protein. Western blotting analysis was performed by standard procedures, as previously described (García-Matas et al., 2008). For details see Supporting information.

**Results**

Representative images of neuron and astrocyte two-dimensional gels after silver staining are shown in Fig. 2. Approximately 900 spots were detected in astrocyte gels and 1200 in the higher resolution neuron gels. The differential proteomics analysis of the neurons of the two mouse strains showed 27 differential spots in SAMP8 as compared to SAMR1. Twenty-four spots were identified by PMF, which are listed in Table 1A. A total of 16 differentially expressed spots were obtained in astrocytes of SAMP8 as compared to SAMR1 mice. All spots were identified by PMF, as listed in Table 1B. MS data for each

spot are summarized in Tables S1A and S1B, for neurons and astrocytes respectively (Supporting information; see also PMF files). All the spots were identified with a high probability-related molecular weight search (MOWSE) score. The Mascot score was used for one mass spectrum (see Table S1A). Multiple differential spots were detected for three neuron proteins: tubulin alpha-1 chain, tubulin alpha-3 chain and tubulin beta-5 chain. This could indicate differential expression in several coexisting posttranslational modifications or isoforms of these proteins. The identified 17 neuron and 14 astrocyte proteins, can functionally be classified as those involved in the energy metabolism of the cell, biosynthetic pathways, transduction and signaling mechanisms, response to cellular stress and cytoskeletal functions. Additionally, one identified astrocyte protein has a transport function and a neuronal protein has an unknown function in mammals.

Densitometric analysis and representative images of Western blot are shown in Fig. S1 (Supporting information). Significant increases in the signaling protein Ppp1ca in neurons and in the stress response protein Aldh2 in astrocytes were in agreement with the proteomic analyses.

Network analyses were performed with 13 neuron and 9 astrocyte differentially expressed proteins, which were connected to other proteins in the HPI (Table 3, Fig. 3). Analytical parameters showed that neuron proteins were closely related, as they were connected by a shorter distance than average in HPI. In addition, much higher centrality parameters and clustering coefficient than the whole HPI indicated that these neuron proteins participate in many relevant cell pathways. The astrocyte protein network showed a higher clustering coefficient and a slight increase in two centrality parameters, that indicate its inclusion in more cell pathways than average in HPI.

## Discussion

The proteomic study of neuron and astrocyte cultures of SAMP8 mouse showed a differential pattern of protein expression alterations as compared to those of the reference strain SAMR1. The function of the proteins involved and the possible significance of the changes are discussed below.

### *Energy metabolism*

There was an increase in acyl-coenzyme A thioesterase 2 expression in both neurons and astrocytes. In addition, a decrease in acyl coenzyme A thioesterase 1 expression was found in neurons. Acyl-coenzyme A thioesterases catalyze the hydrolysis of acyl-coenzyme A to free fatty acids and coenzyme A, providing the potential to regulate intracellular levels of these molecules. Isoform 1 is cytoplasmic and isoform 2 is mitochondrial. Fatty acids and their activated form, acyl-coenzyme A, are key components of numerous metabolic processes of biosynthesis/catabolism of lipids. The enzyme phosphoglycerate mutase 1, which catalyzes the interconversion of 3-phosphoglycerate and 2-phosphoglycerate during glycolysis and gluconeogenesis, showed decreased expression in SAMP8 neuron proteoma. A decrease in this enzyme has been reported in the hippocampus proteoma of AD (Sultana *et al.* 2007) and might be an AD biomarker (Zellner *et al.* 2009). It plays an important role in maintaining synaptic function. A decrease in glycolysis has been related to the abnormally low levels of brain acetylcholine in aged SAMP8 (Poon *et al.* 2004). SAMP8 astrocytes showed an increase in adenylate kinase isoenzyme 4, a phosphotransferase that catalyzes the interconversion of adenine nucleotides and therefore regulates mitochondrial respiration and cytosolic energy metabolism. Astrocyte cultures also showed a significant decrease in the precursor form of cytochrome oxidase (Cox) isoform 4-1. Cox catalyzes the electron transfer from ferrocytochrome *c* to oxygen in the mitochondrial electron transport chain. Isoform IV-1 predominates in brain tissue. Defective energy metabolism in aging and AD has been linked to decreased Cox 4 activity levels (Ojaimi *et al.* 1999; Maurer *et al.* 2000).

*Biosynthesis*

SAMP8 neuron proteoma showed an increase in both enzymes that sequentially catalyze L-serine biosynthesis: D-3-phosphoglycerate dehydrogenase and phosphoserine aminotransferase. L-serine is a building block for the synthesis of proteins and neural phospholipids. Astrocytes showed a decrease in dihydropteridine reductase, an enzyme that is involved in the maintenance of tetrahydrobiopterin levels. The latter is a cofactor in the synthesis of amino acid monooxygenases and nitric oxide production. SAMP8 astrocytes showed a more alkaline form of S-methyl-5-thioadenosine phosphorylase, a pentosyltransferase that participates in adenine and methionine metabolism and in the biosynthesis of polyamines.

*Cell transduction and signaling*

SAMP8 neuron proteoma showed an increase in poly(rC)-binding protein 1 and protein 2, but only poly(rC)-binding protein 1 was increased in astrocytes. These are the two major poly(C)-binding proteins in mammalian cells and mediate a variety of post-transcriptional functions related to mRNA stability and expression. In addition, there were higher levels of Ppp1ca, a specific subunit of a key serine/threonine-protein phosphatase known as type 1 (PP1). Reversible protein phosphorylation is a fundamental mechanism by which many biological functions are regulated. PP1 participates in protein synthesis and long-term synaptic plasticity. It has been shown that PP1 needs to be inhibited to gate long term potentiation, because it limits learning and favors forgetting (Jouvenceau *et al.* 2006). Therefore, PP1 upregulation may contribute to the cognitive deficiencies in SAMP8 mice. Caspase-3 precursor was increased in SAMP8 neurons. This proenzyme urdergoes proteolytic processing after a variety of apoptotic stimuli. It then acts as an effector caspase, and leads to cell apoptosis.

In astrocyte SAMP8 cultures there was an increase in the enzyme protein-arginine deiminase type 2, which catalyzes the conversion of arginine to citrulline. Citrulline is not incorporated into proteins, thus deimination of arginine residues appears to form a post-translational protein modification. Furthermore, this enzyme may be involved in nitric oxide synthesis.

*Stress response proteins*

SAMP8 neuron proteoma showed an increase in erlin-2, also named SPFH domain-containing protein 2. This is a key component of the recently described pathway for endoplasmic reticulum-associated degradation, where it acts as a substrate recognition factor. This pathway accounts for the degradation of aberrant proteins and some other proteins that are metabolically regulated (Pearce *et al.* 2007). The small ubiquitin-like modifier (SUMO)-activating enzyme subunit 1 also increased. This integrates a nuclear and cytoplasmic dimeric enzyme that mediates the ATP-dependent activation of SUMO proteins. It is the first enzyme in the pathway that leads to the formation of ubiquitin-protein conjugates. Therefore, it is rate-limiting in the conjugation and increases in response to oxidative stress. The related ubiquitin-like protein NEDD8 was reported to be overexpressed in aged SAMP8 (Kumar *et al.* 2000). More generally, the ubiquitin/proteasoma pathway is critical for cell survival and repair and is involved in many cellular processes and age-related diseases (Vernace *et al.* 2007). A marked increase in brain ubiquitin has been reported in AD (Wang *et al.* 1991).

In astrocytes, there was an increase in sodium/hydrogen exchanger 5. Sodium/hydrogen exchangers comprise a family of integral plasma or mitochondrial membrane proteins that are involved in a variety of physiological processes, such as pH regulation, volume control and electrolyte transport. Isoform 5 is restricted almost exclusively to the brain. Its increase in SAMP8 could be linked to an increased demand for eliminating acids generated by metabolism under pathophysiological conditions or to counter adverse environmental conditions.

The antioxidant enzyme Aldh2 was increased in the SAMP8 astrocyte proteoma. Aldh2 is involved in the detoxification of reactive aldehydes in the mitochondria. An increase in Aldh2 has been described in the brain of old rats (Cao Danh *et al.* 1983), the olfactory system of aged mice (Poon et *al.* 2005) and in AD temporal cortex (Picklo *et al.* 2001).

*Cytoskeletetal proteins*

Actin cytoplasmic 2 (gamma-actin) was decreased in both SAMP8 neurons and astrocytes. It is present in most cells types as component of the cytoskeleton and mediator of internal cell motility. Tubulin is the major constituent of microtubules and is formed by dimers of alpha and beta chains. The isotypes 1A and 3 of the alpha chain and the 5 isotype of the beta chain were decreased in SAMP8 neurons. The appearance of differential expression in a number of spots for both tubulins is in agreement with the reported high diversity of modifications in cytoskeletal proteins (Verdier-Pinard *et al.* 2003). Disruption of microtubule-based transport and synaptic mechanisms occurs in AD neurons (Butler *et al.* 2007). Decreased tubulin alpha and beta chains have been reported in aged rodent brain (Poon *et al.* 2006; Tsugita *et al.* 2000). To notice that tubulin beta 5 is decreased in AD brain (Shiozaki *et al*. 2004; Sultana et al. 2007) and it might be a cytoskeletal AD biomarker (Zellner *et al.* 2009). Finally, the actin-related protein macrophage capping protein presented reduced expression in the SAMP8 astrocyte proteoma. Macrophage capping protein, discovered in macrophages, is present in a variety of tissues where it binds and caps actin filaments. Deficiency of capping proteins may contribute to derangement of cellular organelle motility in SAMP8. The actin-capping protein F has been described as decreased in fetal Down syndrome brain (Gulesserian *et al.* 2002). The latter was also reduced in aged rat hippocampus (Poon *et al.* 2006). This decreased expression of specific skeleton proteins is in general agreement with the cortical atrophy, axonal dystrophia with a reduction in dentritic spines, and membrane and transport alterations that have been described in SAMP8 brains (Kawamata *et al.* 1998).

Increased cytoskeletal proteins included fascin in neurons and stomatin-like protein 2 and myosin light polypeptide 6 in astrocytes. Fascin is an actin-crosslinking protein that is present in brain. It organizes actin filaments into tightly packed bundles and contributes to the architecture and function of cell protrusions and microfilaments. Stomatin-like protein 2 is an unusual member of the cytoskeletal stomatin family. Recent studies have associated stomatin-like protein 2 with the mitochondrial membranes and the maintenance of mitochondrial morphology (Hájek et al. 2007). Myosin is composed of 2 heavy chains and 4 light chains, where light polypeptide 6 is a regulatory chain. Myosin anchors to actin filaments and induces a movement that is coupled to the hydrolysis of a nucleoside triphosphate.

*Miscellaneous*

Coatomer subunit epsilon was decreased in the SAMP8 mouse astrocyte proteoma. The coatomer is a cytosolic protein complex formed by at least seven subunits. It associates with specific Golgi vesicles to mediate biosynthetic protein transport from the endoplasmic reticulum to the Golgi network. It also mediates retrograde transport of immature or abnormal proteins from Golgi to endoplasmic reticulum. The epsilon subunit plays a structural role in the coatomer complex (Kimata *et al.,* 2000).

The significance of an increase in WD repeat-containing protein 61 in the SAMP8 neuron proteoma has not been clarified to date. The WD-sequence repeat-containing family of proteins is a large family with a wide range of roles in eukaryotic cells. The role of WD repeat protein 61, also known as Rec14, is not yet known in mammalians. In yeast, it is functional in early stages of meiosis.

The proteins that were abnormally expressed in cultures of SAMP8 neurons and astrocytes were associated with pathways similar to those reported as altered in the brain tissue of SAMP8, aged brain or AD brain (Butterfield and Poon, 2005; Galvin and Ginsberg, 2003; Sowell *et al.* 2009). Namely, this study confirms the presence of previously reported neurodegeneration markers such as lower phosphoglycerate mutase 1, Cox 4, and tubulin proteins and higher aldehyde dehydrogenase and ubiquitin-related proteins. Interestingly these markers are detected whether in neurons or astrocytes. On the other hand we can suggest as a new marker an increased PP1 activity, after the increased expression of Ppp1ca in neurons. To highlight the number of mitochondrial proteins with altered expression, both in neurons and astrocytes, this supporting the mitochondrial dysfunction and oxidative

stress in SAMP8 brain. Genomic studies of SAMP8 brain also found that genes related to mitochondria are abnormally expressed, in addition to cytoskeletal, neurotrophic and signaling-related genes (for revision see Tomobe and Nomura, 2009). According to our network analysis, many proteins affected in neurons belong to more crucial and complex pathways than those in astrocytes and their alteration may be highly disruptive of cognitive processes. In addition, astrocyte protein alterations are in agreement with their functional and neuroprotective capacity loss (García-Matas *et al.* 2008). We have to take into account the limitation of the proteomic approach where only abundant soluble proteins are detected and can be reliably compared between SAMR1 and SAMP8, and that the degree of variation for the different proteins is generally low. Nonetheless, the proteomic study of neuron and astrocyte cultures demonstrated that both cells types are implicated in the brain protein pathway alterations of the SAMP8 mouse model of age-related neurodegeneration, and that these alterations can be modeled in vitro.

**Acknowledgments**

This study was supported by grants SAF2006-13092-C02-02 from the Spanish Ministerio de Ciencia e Innovación, RD06/0013/1004 (RETICEF) from the Instituto de Salud Carlos III and DURSI 2005/SGR/00826 from the Generalitat (Autonomous Government of Catalonia). S. García-Matas received a Generalitat fellowship. We thank J. López Regal and A. Parull for their skilful technical assistance. We thank G. Sanchez for his assistance. The Proteomics Laboratory CSIC/UAB is a member of ProteoRed, funded by Genoma Spain, and follows the quality criteria set up by ProteoRed standards. The authors declare that there are no financial or commercial conflicts of interest.

**References**


Butler D., Bendiske J., Michaelis M.L., Karanian D.A. and Bahr B.A. (2007) Microtubule stabilizing agent prevents protein accumulation-induced loss of synaptic markers. *Eur. J. Pharmacol*. **562,** 20-27.

Butterfield D.A., Howard B.J., Yatin S., Allen K.L. and Carney J.M. (1997) Free radical oxidation of brain proteins in accelerated senescence and its modulation by N-tert-butyl-alpha-phenylnitrone. *Proc. Natl. Acad. Sci. USA* **94,** 674-678.

Butterfield D.A. and Poon H.F. (2005) The senescence-accelerated prone mouse (SAMP8): a model of age-related cognitive decline with relevance to alterations of the gene expression and protein abnormalities in Alzheimer's disease. *Exp. Gerontol.* **40**, 774-783.



Butterfield D.A., Howard B.J., Yatin S., Allen K.L. and Carney J.M. (1997) Free radical oxidation of brain proteins in accelerated senescence and its modulation by N-tert-butyl-alpha-phenylnitrone. *Proc. Natl. Acad. Sci. USA* **94,** 674-678.



Butler D., Bendiske J., Michaelis M.L., Karanian D.A. and Bahr B,A. (2007) Microtubule stabilizing agent prevents protein accumulation-induced loss of synaptic markers. *Eur. J. Pharmacol*. **562,** 20-27.

Canudas A.M., Gutiérrez-Cuesta J., Rodríguez M.I., Acuña-Castroviejo D., Sureda F.X., Camins A. and Pallàs M. (2005) Hyperphosphorylation of microtubule-associated protein tau in senescence-accelerated mouse (SAM). *Mech. Ageing Dev*. **126,** 1300-1304.

Cao Danh H., Strolin Benedetti M. and Dostert P. (1983) Age-related changes in aldehyde dehydrogenase activity of rat brain, liver, and heart. *J. Neurochem*. **41,** 618-622.

Farr S.A., Poon H.F., Dogrukol-Ak D., Drake J., Banks W.A., Eyerman E., Butterfield D.A. and Morley J.E. (2003) The antioxidants alpha-lipoic acid and N-acetylcysteine reverse memory impairment and brain oxidative stress in aged SAMP8 mice. *J. Neurochem.* **84,** 1173-1183.

Flood J.F. and Morley J.E. (1998) Learning and memory in the SAMP8 mouse. *Neurosci. Biobehav. Rev.* **22,**1-20.

Frandsen A. and Schousboe A. (1990) Development of excitatory amino acid induced cytotoxicity in cultured neurons. *Int. J. Dev. Neurosci*. **8,** 209–216.

Fujibayashi Y., Yamamoto S., Waki A., Konishi J. and Yonekura Y. (1998) Increased mitochondrial DNA deletion in the brain of SAMP8, a mouse model for spontaneous oxidative stress brain. *Neurosci. Lett.* **254,** 109-112.

Galvin J.E. and Ginsberg S.D. (2003) Expression profiling in the aging brain: A perspective. *Ageing Res. Rev*. **4,** 529-547.

García-Matas S., Gutiérrez-Cuesta J., Coto-Montes A., Rubio-Acero R., Díez-Vives C., Camins A., Pallàs M., Sanfeliu C. and Cristòfol R. (2008) Dysfunction of astrocytes in the senescence-accelerated mice SAMP8 reduces their neuroprotective capacity. *Aging Cell* **7,** 630-640.

Gulesserian T., Kim S.H., Fountoulakis M. and Lubec G. (2002) Aberrant expression of centractin and capping proteins, integral constituents of the dynactin complex, in fetal Down syndrome brain. *Biochem. Biophys. Res. Commun*. **291,** 62-67.

Hájek P., Chomyn A. and Attardi G. (2007) Identification of a novel mitochondrial complex containing mitofusin 2 and stomatin-like protein 2. *J. Biol. Chem*. **282,** 5670-5681.

Jouvenceau A., Hédou G., Potier B., Kollen M., Dutar P. and Mansuy I.M. (2006) Partial inhibition of PP1 alters bidirectional synaptic plasticity in the hippocampus. *Eur. J. Neurosci*. **24,** 564-572.

Kawamata T., Akiguchi I., Maeda K., Tanaka C., Higuchi K, Hosokawa M. and Takeda T. (1998) Age-related changes in the brains of senescence-accelerated mice (SAM): Association with glial and endothelial reactions. *Microsc. Res. Tech*. **43,** 59-67.

Kimata Y., Higashio H., Kohno K. (2000) Impaired proteasome function rescues thermosensitivity of yeast cells lacking the coatomer subunit epsilon-COP. *J. Biol. Chem.* **275,** 10655-10660.

Kumar V.B., Franko M.W., Farr S.A., Armbrecht J. and Morley J.E. (2000) Identification of age-dependent changes in expression of senescence-accelerated mouse (SAMP8) hippocampal proteins by expression array analysis. *Biochem. Biophys. Res. Commun*. **272,** 657-661.

Lü L., Li J., Yew D.T., Rudd J.A., Mak YT. (2008) Oxidative stress on the astrocytes in culture derived from a senescence accelerated mouse strain. *Neurochem. Int.* **52**, 282-289.

Lü L., Mak Y.T., Fang M., Yew D.T. (2009) The difference in gliosis induced by β-amyloid and Tau treatments in astrocyte cultures derived from senescence accelerated and normal mouse strains. *Biogerontology*, in press. [Published online, DOI: 10.1007/s10522-009-9217-3].

Maurer I., Zierz S. and Möller H.-J. (2000) A selective defect of cytochrome c oxidase is present in brain of Alzheimer disease patients. *Neurobiol. Aging* **21,** 455-462.

Mishra, G.R., Suresh M., Kumaran K. *et al.* (2006) Human protein reference database - 2006 update. *Nucleic Acids Res*, **34,** D411-D414.

Morley J.E., Farr S.A., Kumar V.B. and Banks W.A. (2002) Alzheimer's disease through the eye of a mouse. Acceptance lecture for the 2001 Gayle A. Olson and Richard D. Olson prize. *Peptides* **23,** 589-599.

Nabeshi H., Oikawa S., Inoue S., Nishino K. and Kawanishi S. (2006) Proteomic analysis for protein carbonyl as an indicator of oxidative damage in senescence-accelerated mice. *Free Radic. Res.* **40,** 1173-1181.

Ojaimi J., Masters C.L., McLean C., Opeskin K., McKelvie P. and Byrne E. (1999) Irregular distribution of cytochrome c oxidase protein subunits in aging and Alzheimer's disease. *Ann. Neurol.* **46,** 656-660.

Pallas M., Camins A., Smith M.A., Perry G., Lee H. and Casadesus G. (2008) From aging to Alzheimer's disease: Unveiling "the switch" with the senescence-accelerated mouse model (SAMP8). *J. Alzheimers Dis.* **15,** 615-624.

Pearce M.M.P., Wang Y., Kelley G.G. and Wojcikiewicz R.J.H. (2007) SPFH2 mediates the endoplasmic reticulum-associted degradation of inositol 1,4,5-triphosphate receptors and other substrates in mamalian cells. *J. Biol. Chem*. **282,** 20104-20115.

Picklo M.J., Olson S.J., Markesbery W.R. and Montine T.J. (2001) Expression and activities of aldo-keto oxidoreductases in Alzheimer disease. *J. Neuropathol. Exp. Neurol*. **60,** 686-695.

Poon H.F., Castegna A., Farr S.A., Thongboonkerd V., Lynn B.C., Banks W.A., Morley J.E., Klein J.B. and Butterfield D.A. (2004) Quantitative proteomics analysis of specific protein expression and oxidative modification in aged senescence-accelerated-prone 8 mice brain. *Neuroscience* **126,** 915-928.

Poon H.F., Vaishnav R.A. Butterfield D.A., Getchell M.L. and Getchell T.V. (2005) Proteomic identification of differentially expressed proteins in the aging murine olfactory system and transcriptional analysis of the associated genes. *J. Neurochem*. **94,** 380-392.

Poon H.F., Calabrese V., Calvani M. and Butterfield A. (2006) Proteomic analyses of specific protein oxidation and protein expression in aged rat brain and its modulation by L-acetylcarnitine: insights into the mechanisms of action of this proposed therapeutic agent for CNS disorders associated with oxidative stress. *Antioxid. Redox Signal*. **8,** 381-394.

Quero C., Colomé N., Prieto M.R., Carrascal M., Posada M., Gelpí E. and Abian J. (2004) Determination of protein markers in human serum: Analysis of protein expression in toxic oil syndrome. *Proteomics* **4,** 303-315.

Ramirez-Boo M., Garrido J.J., Ogueta S., Calvete J.J., Gómez-Díaz C., Moreno A. (2006) Analysis of porcine peripheral blood mononuclear cells proteome by 2-DE and MS: Analytical and biological variability in the protein expression level and protein identification. *Proteomics* **6,** S215-S225.

Shevchenko A., Wilm M., Vorm O. and Mann M. (1996) Mass spectrometric sequencing of proteins from silver-stained polyacrylamide gels. *Anal. Chem.* **68,** 850-858.

Shiozaki A., Tsuji T., Kohno R., Kawamata J., Uemura K., Teraoka H. and Shimohama S. (2004) Proteome analysis of brain proteins in Alzheimer's disease: subproteomics following sequentially extracted protein preparation. *J Alzheimers Dis* **6,** 257-268.

Sowell R.A., Joshua B.O. and Butterfield D.A. (2009) Proteomics in animal models of Alzheimer's and Parkinson's diseases. *Ageing Res. Rev.* **8,** 1-17.

Sultana R., Boyd-Kimball D., Cai J., Pierce W.M. Klein J.B., Merchant M. and Butterfield D.A. (2007) Proteomics analysis of the Alzheimer's disease hippocampal proteome. *J. Alzeimers. Dis.* **11,** 153-164.

Sureda F.X., Gutiérrez-Cuesta J., Romeu M., Mulero M., Canudas A.M., Camins A., Mallol J. and Pallàs M. (2006) Changes in oxidative stress parameters and neurodegeneration markers in the brain of the senescence-accelerated mice SAMP8. *Exp. Gerontol.* **41**, 360-367.

Takeda T. (1999) Senescence-accelerated mouse (SAM): a biogerontological resource in aging research. *Neurobiol. Aging* **20,** 105-110.

Takeda T. (2009) Senescence-accelerated mouse (SAM) with special references to neurodegeneration models, SAMP8 and SAMP10. *Neurochem. Res.* **34,** 639-659.

Takemura M., Nakamura S., Akiguchi I., Ueno M., Oka N., Ishikawa S., Shimada A., Kimura J. and Takeda T., 1993) β/A4 Proteinlike immunoreactive granular structures in the brain of senescence-accelerated mouse. *Am. J. Pathol.* **142,** 1887-1897.

Tomobe K. and Nomura Y. (2009) Neurochemistry, neuropathology, and heredity in SAMP8: a mouse model of senescence. *Neurochem. Res*. **34,** 660-669.

Tsugita A., Kawakami T., Uchida T., Sakai T., Kamo M., Matsui T., Watanabe Y., Morimasa T., Hosokawa K. and Toda T. (2000) Proteoma analysis of mouse brain: Two-dimensional electrophoresis profiles of tissue proteins during the course of aging. *Electrophoresis* **21,** 1853-1871.

Vernace V.A., Schmidt-Glenewinkel T. and Figueiredo-Pereira M.E. (2007) Aging and regulated protein degradation: who has the UPPer hand? *Aging Cell* **6**, 599-606.

Verdier-Pinard P., Wang F., Martello L., Burd B., Orr G.A. and Horwitz S.B. (2003) Analysis of tubulin isotypes and mutations from taxol-resistant cells by combined isoelectrofocusing and mass spectrometry. *Biochemistry* **42,** 5349-5357.

Wang G.P., Khatoon S., Iqbal K. and Grundke-Iqbal I. (1991) Brain ubiquitin is markedly elevated in Alzheimer disease. *Brain Res*. **566,** 146-151.

Wang Q., Liu Y., Zou X., Wang Q., An M., Guan X., He J., Tong Y. and Ji J. (2008) The hippocampal proteomic analysis of senescence-accelerated mouse: Implications of Uchl3 and mitofilin in cognitive disorder and mitochondria dysfunction in SAMP8. *Neurochem. Res.* **32,** 1776-1782.

Zellner M., Veitinger M. and Umlauf E. (2009) The role of proteomics in dementia and Alzheimer's disease. *Acta Neuropathol*. **118,** 181-195.

Table 1A Differentially expressed proteins in neuron cultures of SAMR1 and SAMP8

| **Protein function** | **Protein identified** | **Gene name** | **Change** SAMP8 vs. SAMR1 | **SAMR1** mean ± SD | **SAMP8** mean ± SD | **Ratio** SAMR1/ SAMP8 | ***p*** | **Spot** |
|---|---|---|---|---|---|---|---|---|
| ***Energy metabolism*** | Acyl-coenzyme thioesterase 2 | Acot2 | Up | ND | 0.040 ± 0.011 | NA | NA | 1162 |
| | Phosphoglycerate mutase 1 | Pgam1 | Down | 0.080 ± 0.054 | 0.029 ± 0.012 | 2.8 | 0.0211 | 1140 |
| | Acyl-coenzyme thioesterase 1 | Acot1 | Down | 0.048 ± 0.015 | ND | NA | NA | 1120 |
| ***Biosynthesis*** | D-3-phosphoglycerate dehydrogenase | Phgdh | Up | 0.357 ± 0.198 | 0.719 ± 0.184 | 0.5 | 0.0014 | 188 |
| | Phosphoserine aminotransferase | Psat1 | Up | 0.161 ± 0.080 | 0.324 ± 0.160 | 0.5 | 0.0164 | 542 |
| ***Transduction and signaling*** | Poly(rC)-binding protein 2 | Pcbp2 | Up | 0.089 ± 0.044 | 0.239 ± 0.114 | 0.4 | 0.0036 | 565 |
| | Serine/threonine-protein phosphatase PP1-alpha catalytic subunit | Ppp1ca | Up | 0.064 ± 0.034 | 0.140 ± 0.058 | 0.5 | 0.0036 | 557 |
| | Caspase-3 | Casp3 | Up | 0.081 ± 0.022 | 0.154 ± 0.075 | 0.5 | 0.0130 | 765 |
| | Poly(rC)-binding protein 1 | Pcbp1 | Up | 0.102 ± 0.044 | 0.194 ± 0.032 | 0.5 | 0.0001 | 478 |
| ***Stress response*** | Erlin-2 | Erlin2 | Up | 0.058 ± 0.022 | 0.138 ± 0.056 | 0.4 | 0.0011 | 442 |
| | SUMO-activating enzyme subunit 1 | Sae1 | Up | 0.077 ± 0.035 | 0.172 ± 0.030 | 0.4 | 0.0000 | 496 |
| ***Cytoskeletal*** | Fascin | Fscn1 | Up | 0.095 ± 0.048 | 0.230 ± 0.120 | 0.4 | 0.0070 | 228 |
| | Tubulin alpha-3 chain | Tuba3a | Down | 0.116 ± 0.057 | 0.059 ± 0.031 | 2.0 | 0.0256 | 917 |
| | | | Down | 0.108 ± 0.033 | ND | NA | NA | 1156 |
| | Actin, cytoplasmic 2 | Actg | Down | 0.109 ± 0.073 | 0.044 ± 0.014 | 2.5 | 0.0027 | 503 |
| | Tubulin alpha-1A chain | Tuba1a | Down | 0.052 ± 0.031 | 0.024 ± 0.009 | 2.2 | 0.0191 | 1160 |
| | | | | 0.277 ± 0.160 | 0.126 ± 0.062 | 2.2 | 0.0180 | 999 |
| | | | | 0.093 ± 0.041 | 0.040 ± 0.012 | 2.3 | 0.0192 | 444 |
| | | | | 0.068 ± 0.027 | 0.026 ± 0.010 | 2.6 | 0.0004 | 1161 |
| | | | | 0.118 ± 0.033 | 0.034 ± 0.016 | 3.5 | 0.0001 | 494 |
| | | | | 0.230 ± 0.125 | 0.061 ± 0.032 | 3.8 | 0.0066 | 700 |
| | Tubulin beta-5 chain | Tubb5 | Down | 0.115 ± 0.052 | 0.049 ± 0.020 | 2.3 | 0.0042 | 889 |
| | | | | 0.207 ± 0.101 | 0.066 ± 0.040 | 3.1 | 0.0151 | 649 |

| | | | | | | | | |
|---|---|---|---|---|---|---|---|---|
| ***Miscellaneous*** | WD repeat-containing protein 61 | Wdr61 | Up | 0.063 ± 0.025 | 0.120 ± 0.026 | 0.5 | 0.0004 | 709 |

Note: The normalized mean volumes of SAMR1 and SAMP8 differential protein spots and its ratio are indicated along with the changes shown by SAMP8. Normalized volumes were compared using a Student's *t*-test. Protein parameters are described in Supporting information Table S1A.

ND, not detectable; NA, not applicable.

Table 1B Differentially expressed proteins in astrocyte cultures of SAMR1 and SAMP8

| **Protein type** | **Protein identified** | **Gene name** | **Change** SAMP8 vs. SAMR1 | **SAMR1** mean ± SD | **SAMP8** mean ± SD | **Ratio** SAMR1/ SAMP8 | ***p*** | **Spot** |
|---|---|---|---|---|---|---|---|---|
| ***Energy metabolism*** | Adenylate kinase isoenzyme 4 | Ak3l1 | Up | ND | 0.069 ± 0.029 | NA | NA | 671 |
| | Acyl-coenzyme A thioesterase 2 | Acot2 | Up | ND | 0.149 ± 0.020 | NA | NA | 273 |
| | Cytochrome c oxidase subunit 4 isoform 1 | Cox4i1 | Down | 0.054 ± 0.018 | 0.018 ± 0.010 | 3.0 | 0.0353 | 970 |
| ***Biosynthesis*** | Dihydropteridine reductase | Qdpr | Down | 0.741 ± 0.187 | 0.340 ± 0.110 | 2.2 | 0.0330 | 634 |
| | S-methyl-5'-thioadenosine phosphorylase | Mtap | Increased *pI* | 0.119 ± 0.033 | 0.092 ± 0.025 | NA | NA | 604 [a] 1088 |
| ***Transduction and signaling*** | Protein-arginine deiminase type-2 | Padi2 | Up | ND | 0.090 ± 0.003 | NA | NA | 412 |
| | Poly(rC)-binding protein 1 | Pcbp1 | Up | 0.108 ± 0.050 | 0.234 ± 0.047 | 0.5 | 0.0011 | 336 |
| ***Stress response*** | Sodium/hydrogen exchanger 5 | Slc9a5 | Up | ND | 0.075 ± 0.021 | NA | NA | 364 |
| | Aldehyde dehydrogenase, | Aldh2 | Up | 0.056 ± 0.016 | 0.106 ± 0.033 | 0.5 | 0.0333 | 597 |
| ***Cytoskeletal*** | Stomatin-like protein 2 | Stoml2 | Up | 0.075 ± 0.021 | 0.159 ± 0.065 | 0.5 | 0.0134 | 361 |
| | Myosin light polypeptide 6 | Myl6 | Up | 0.833 ± 0.305 | 1.527 ± 0.551 | 0.5 | 0.0224 | 903 |
| | Macrophage-capping protein | Capg | Down | 0.138 ± 0.017 | 0.061 ± 0.024 | 2.3 | 0.0002 | 1075 |
| | Actin, cytoplasmic 2 | Actg | Down | 0.123 ± 0.071 | 0.039 ± 0.022 | 3.2 | 0.0402 | 969 |
| ***Miscellaneous*** | Coatomer subunit epsilon | Cope | Down | 0.529 ± 0.126 | 0.254 ± 0.027 | 2.1 | 0.0053 | 500 |

Note: The normalized mean volumes of SAMR1 and SAMP8 differential protein spots and its ratio are indicated along with the changes shown by SAMP8. Normalized volumes were compared using a Student's *t*-test. Protein parameters are described in Supporting information Table S1B.

[a]First spot number for SAMR1 and second for SAMP8.

ND, not detectable; NA, not applicable.

Table 2 Network analysis of differentially expressed SAMP8 neuron and astrocyte proteins

| | **Average distance** | **Closeness centrality** | **Degree centrality** | **Betweenness centrality** | **Clustering coefficient** |
|---|---|---|---|---|---|
| Neuron nodes n=13 | 3.06 (1-4) | 0.272 (0.229-0.330) | 26.3 (2-125) | 0.0021 (0.0000-0.0139) | 0.177 (0-0.5) |
| Astrocyte nodes n=9 | 4.61 (2-8) | 0.229 (0.143-0.283) | 9.6 (1-37) | 0.0005 (0.0000-0.0025) | 0.160 (0-0.5) |
| HPI nodes n=9047 | 4.26 (1-14) | 0.239 (0.103-0.354) | 7.7 (1-248) | 0.0004 (0.0000-0.0415) | 0.106 (0-1) |

Note: Network analysis was performed for the proteins included in the largest connected component of the Interactome of the Human Protein Reference Database (HPI) as described in Methods. Neuron proteins were: Phosphoglycerate mutase 1; D-3-Phosphoglycerate dehydrogenase; Poly(rC)-binding protein 2; Serine/threonine-protein phosphatase PP1-alpha catalytic subunit; Caspase-3; Poly(rC)-binding protein 1; SUMO-activating enzyme subunit 1; Fascin; Tubulin alpha-3 chain; Actin cytoplasmic 1; Tubulin alpha-1A chain; Tubulin beta-5 chain; WD repeat-containing protein 61. Astrocyte proteins were: Cytochrome c oxidase subunit 4 isoform 1; S-methyl-5'-thioadenosine phosphorylase; Poly(rC)-binding protein 1; Sodium/hydrogen exchanger 5; Aldehyde dehydrogenase; Stomatin-like protein 2; Myosin light polypeptide 6; Actin cytoplasmic 1; Coatomer subunit epsilon. Results are presented as the average value and maximum and minimum values in parentheses.

**Figure legends**

Fig. 1. Flow chart outlining the experimental design and the progression of the proteomic study in SAMR1 and SAMP8 neuron and astrocyte cultures. See text for details.

Fig. 2. Representative images of silver stained two-dimensional gels of neuron (A) and astrocyte cultures (B). Reference number of identified differential spots is indicated for both cell types. Gels were obtained as described in Methods.

Fig. 3. Neuron (A) and astrocyte (B) interacting protein networks for differentially expressed proteins in SAMP8 versus SAMR1. Connecting line thickness indicates proximity: 1, direct connection; 2, 3 and 4 connected through 1, 2 and 3 intermediate nodes, respectively; absence of line, connected through 4 intermediate nodes. Blue box indicates a decrease of SAMP8 versus SAMR1 protein expression; red box indicates an increase; grey box indicates a change of *pI*. Proteins are represented by their gene names, which are listed in Tables 1A and 1B.

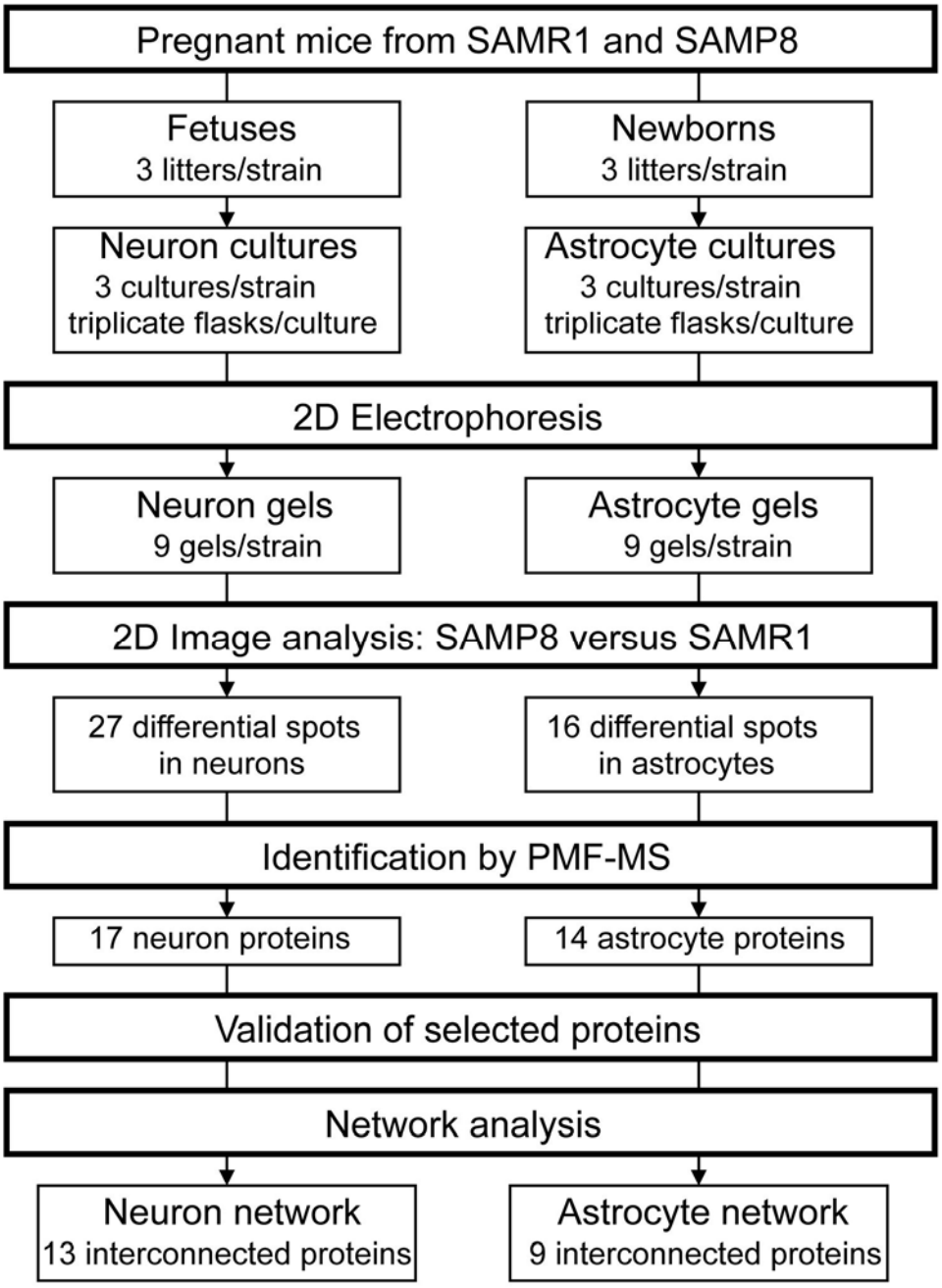
Pregnant mice from SAMR1 and SAMP8
Fetuses
3 litters/strain
Newborns
3 litters/strain
Neuron cultures
3 cultures/strain
triplicate flasks/culture
Astrocyte cultures
3 cultures/strain
triplicate flasks/culture
2D Electrophoresis
Neuron gels
9 gels/strain
Astrocyte gels
9 gels/strain
2D Image analysis: SAMP8 versus SAMR1
27 differential spots
in neurons
16 differential spots
in astrocytes
Identification by PMF-MS
17 neuron proteins
14 astrocyte proteins
Validation of selected proteins
Network analysis
Neuron network
13 interconnected proteins
Astrocyte network
9 interconnected proteins

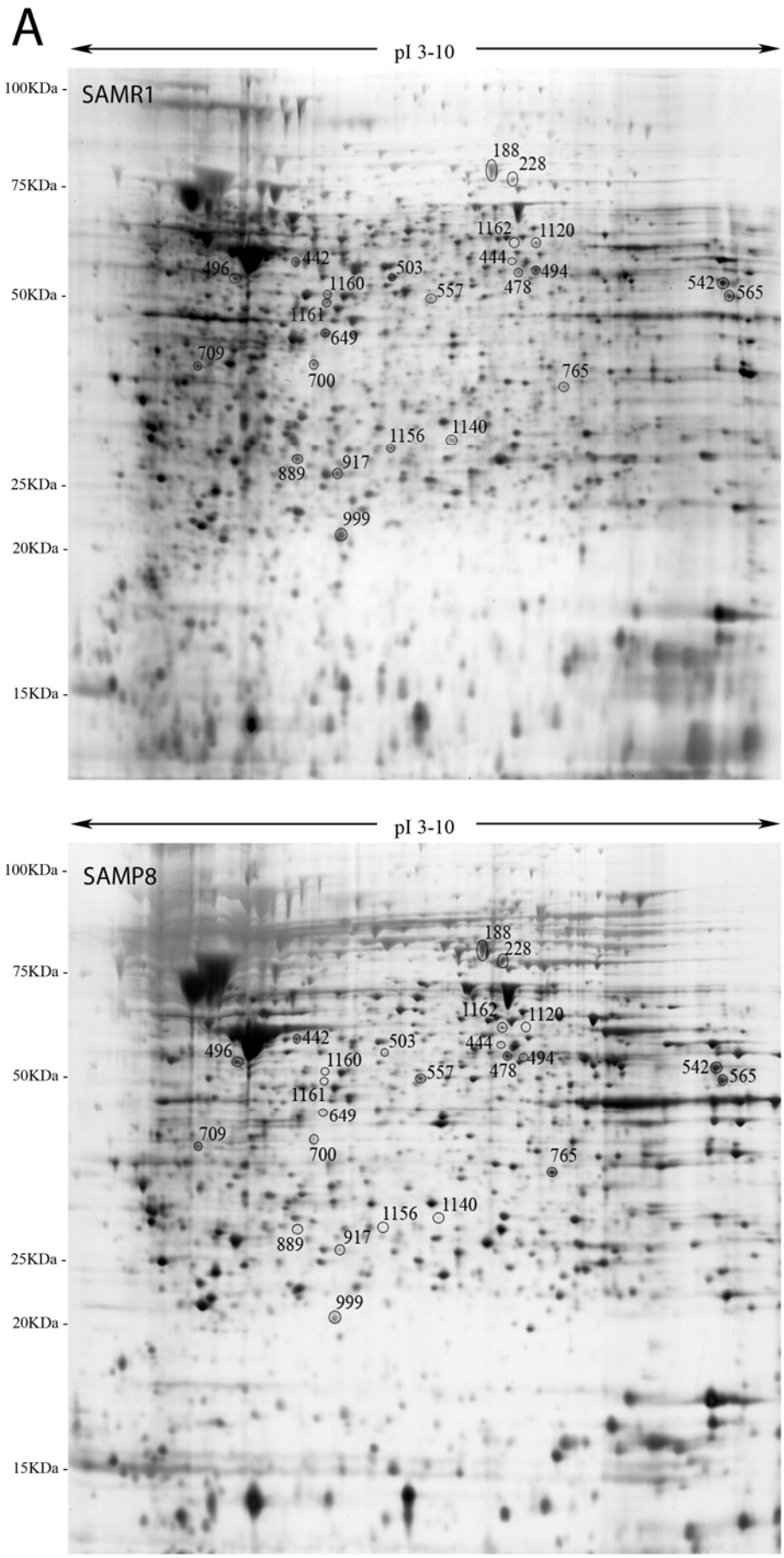
A
pI 3-10
100KDa
SAMR1
75KDa
50KDa
25KDa
20KDa
15KDa
188
228
1162
1120
444
494
496
442
503
1160
557
478
542
565
1161
649
709
700
765
1156
1140
889
917
999
pI 3-10
100KDa
SAMP8
75KDa
50KDa
25KDa
20KDa
15KDa
188
228
1162
1120
444
494
496
442
503
1160
557
478
542
565
1161
649
709
700
765
1156
1140
889
917
999

B

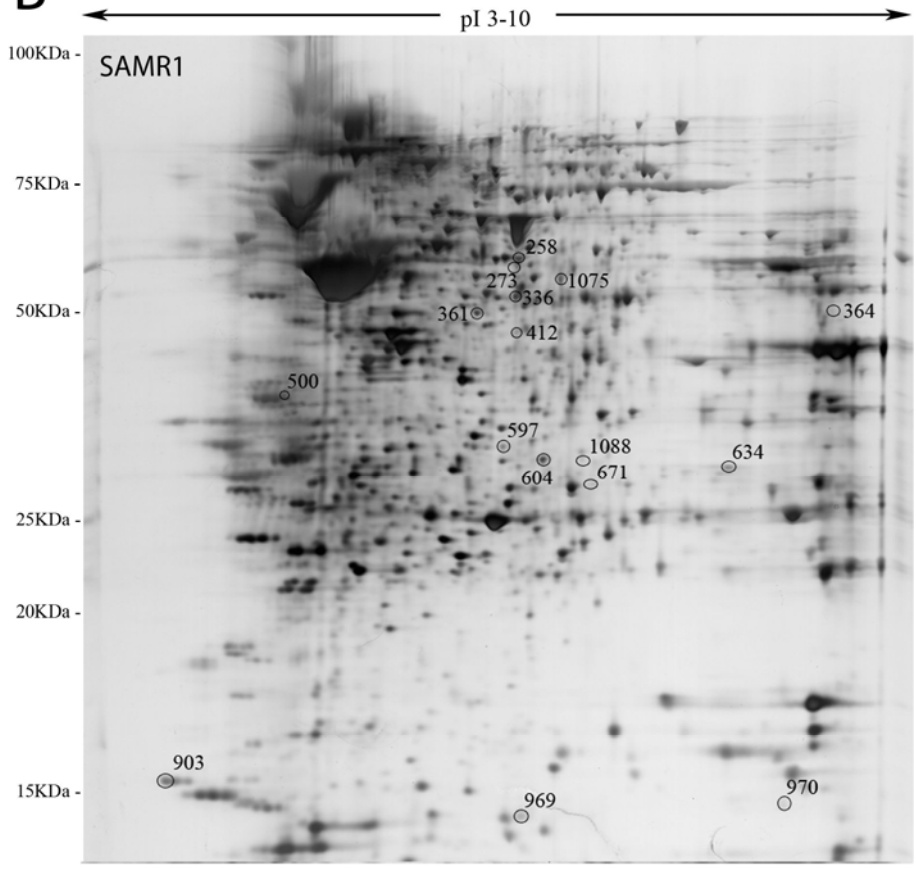
pI 3-10
100KDa -
SAMR1
75KDa -
50KDa -
25KDa -
20KDa -
15KDa -
258
273
1075
336
361
364
412
500
597
1088
634
604
671
903
969
970

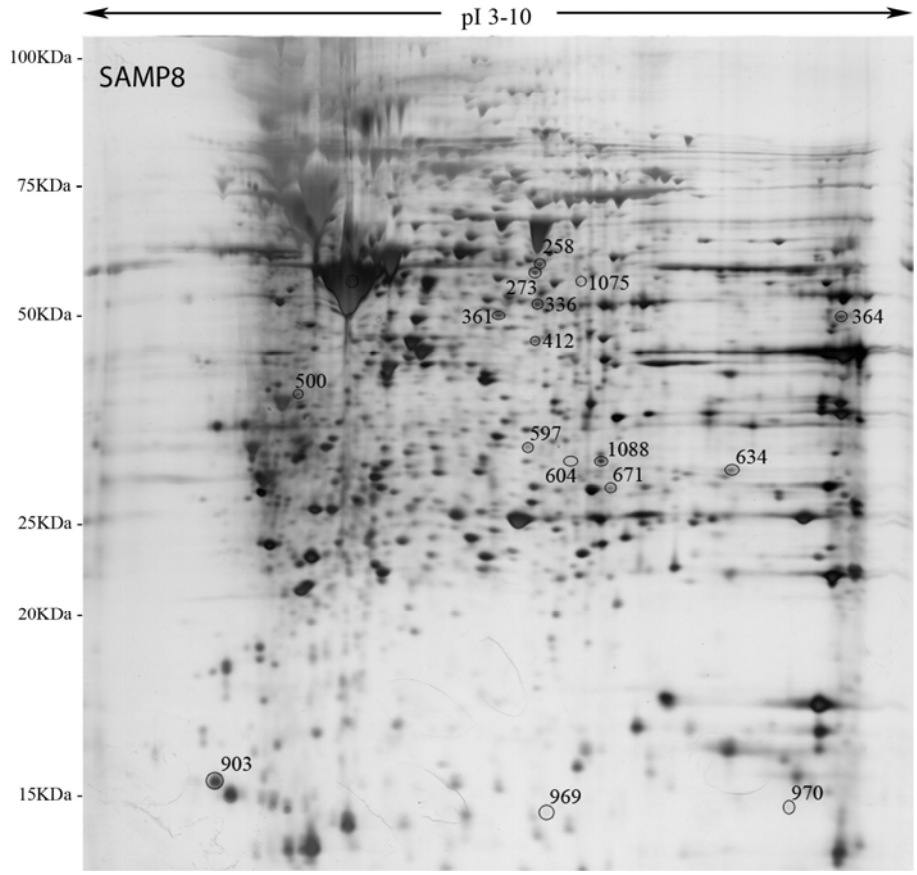
pI 3-10
100KDa -
SAMP8
75KDa -
50KDa -
25KDa -
20KDa -
15KDa -
258
273
1075
336
361
364
412
500
597
1088
634
604
671
903
969
970

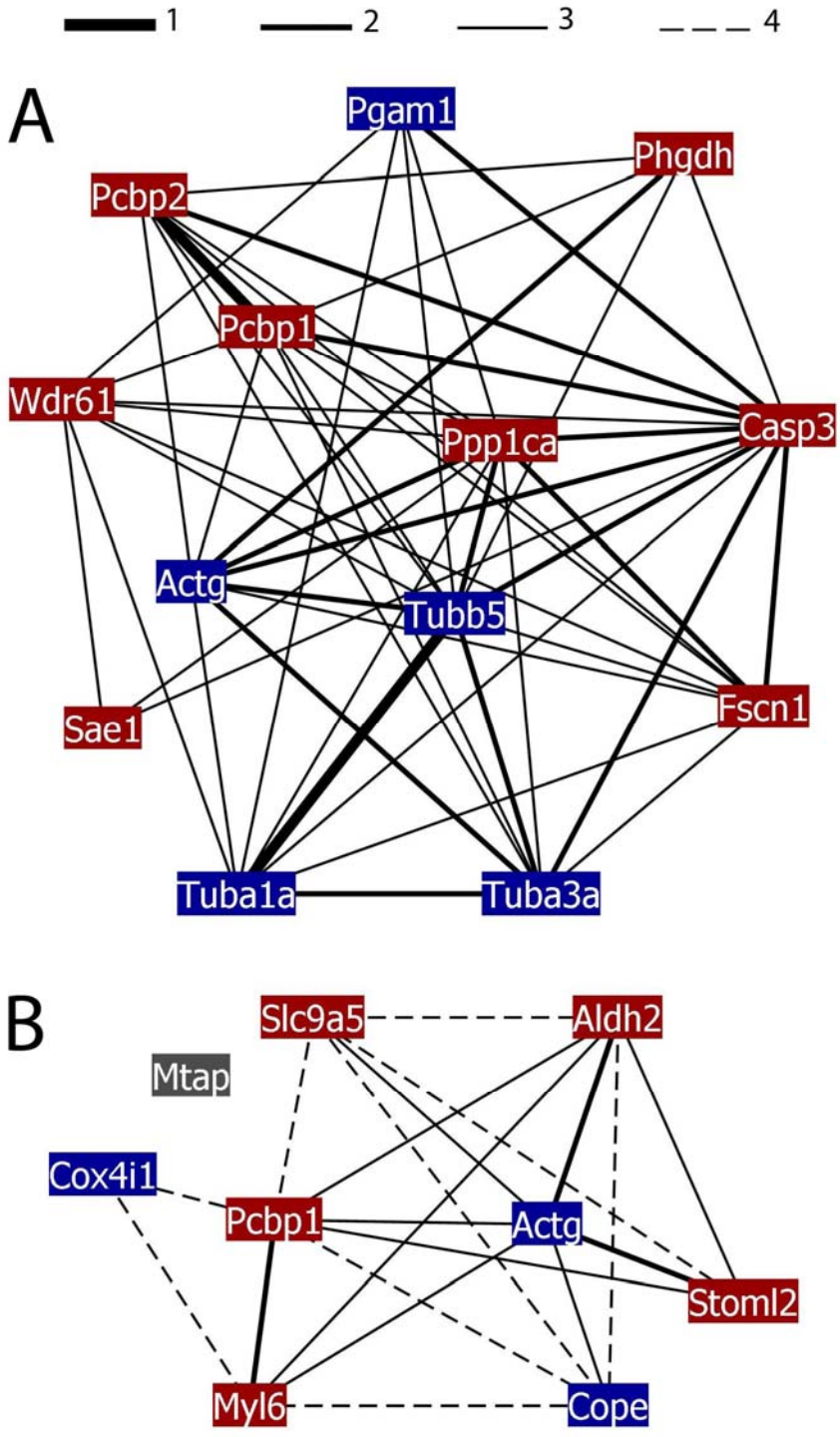
1
2
3
4
A
Pgam1
Phgdh
Pcbp2
Pcbp1
Wdr61
Casp3
Ppp1ca
Actg
Tubb5
Fscn1
Sae1
Tuba1a
Tuba3a
B
Slc9a5
Aldh2
Mtap
Cox4i1
Pcbp1
Actg
Stoml2
Myl6
Cope

**Díez-Vives et al. 2009, Supporting information**

## Western blotting method

Cultured cells were lysed for 10 min on ice in RIPA buffer containing a protease inhibitor cocktail (Complete, Roche, Basel, Switzerland) and 1 mM orthovanadate. They were collected, sonicated to further lyse the cells, and centrifuged. The supernatants were frozen at –20ºC until assay. Proteins were quantified by the Bradford method and 15 μg of protein extracts were denatured, loaded onto a SDS-polyacrylamide gel and electrophoresed. Proteins were transferred onto polyvinylidene fluoride membranes (Immobilon-P, Millipore, Bedford, MA). Neuron membranes were incubated with anti-PP1-alpha catalytic subunit (Ppp1ca) (Cell Signaling, Danvers, MA) and astrocyte ones with anti-aldehyde dehydrogenase (Aldh2) (Santa Cruz Biotechnology, Santa Cruz, CA), diluted 1:1,000. Membranes were then incubated with horseradish peroxidase conjugated secondary antibodies. Proteins were detected with a chemiluminescence detection system, based on the luminol reaction. Densitometric analysis of the digitalized immunoreactive bands was performed using Quantity One software (Bio Rad). The levels of protein immunoreactivity were normalized to that of glyceraldehyde 3-phosphate dehydrogenase (GAPDH) by incubation with anti-GAPDH (Assay Designs, Ann Harbor, MI) 1:5,000.

## Western blotting results

Legend for Fig. S1. Representative immunoblots and densitometric analysis of selected proteins differentially expressed in SAMP8 (P8) and SAMR1 (R1) neuron or astrocyte cultures. Levels of Ppp1ca in neurons (A) and Aldh2 in astrocytes (B). *$p<0.05$, Student's *t*-test.

**Mass spectrometry (MS) data for the differential spots**

Table S1A Identification of proteins by MALDI-TOF MS in the two-dimensional gels of SAMR1 and SAMP8 neurons

| **Protein identified** | **Swiss-Prot Acc. No.** | **Theoretical** | | **Experimental** | | **Match Pept.** No. | **Seq cover** % | **MOWSE score** | **Spot** |
|---|---|---|---|---|---|---|---|---|---|
| | | **Mr** KDa | **p*I*** | **Mr** KDa | **p*I*** | | | | |
| Acyl-coenzyme A thioesterase 2 | Q9QYR9 | 50 | 6.9 | 58 | 6.7 | 8 | 26 | 2.06E+06 | 1162 |
| Phosphoglycerate mutase 1 | Q9DBJ1 | 29 | 6.7 | 26 | 6.3 | 8 | 50 | 4.00E+05 | 1140 |
| Acyl-coenzyme A thioesterase 1 | O55137 | 46 | 6.1 | 58 | 7.0 | 5 | 16 | 9.81E+03 | 1120 |
| D-3-phosphoglycerate dehydrogenase | Q61753 | 57 | 6.1 | 77 | 6.1 | 15 | 30 | 1.21E+08 | 188 |
| Phosphoserine aminotransferase | Q99K85 | 40 | 8.2 | 49 | 9.3 | 15 | 37 | 7.02E+08 | 542 |
| Poly(rC)-binding protein 2 | Q61990 | 38 | 6.3 | 51 | 9.4 | 8 | 28 | 9.58E+04 | 565 |
| Serine/threonine-protein phosphatase PP1-alpha catalytic subunit | P62137 | 38 | 5.9 | 49 | 6.2 | 10 | 38 | 5.26E+07 | 557 |
| Caspase-3 | P70677 | 31 | 6.4 | 35 | 7.1 | 4 | 19 | 6.71E+02 | 765 |
| Poly(rC)-binding protein 1 | P60335 | 37 | 6.7 | 50 | 6.8 | 5 | 23 | 2.82E+04 | 478 |
| Erlin-2 | Q8BFZ9 | 38 | 5.4 | 57 | 5.2 | 6 | 17 | 7.50E+03 | 442 |
| SUMO-activating enzyme subunit 1 | Q9R1T2 | 39 | 5.2 | 50 | 4.7 | 13 | 52 | 1.28E+08 | 496 |
| Fascin | Q61553 | 54 | 6.2 | 75 | 6.8 | 9 | 24 | 1.81E+05 | 228 |
| Tubulin alpha-3 chain | P05214 | 50 | 5.0 | 24 | 6.9 | 6 | 17 | 9.04E+04 | 1156 |
| | | | | 24 | 6.0 | 4 | 8 | 1.48E+02 | 917 |
| Actin, cytoplasmic 2 | P63260 | 42 | 5.3 | 50 | 6.8 | 9 | 40 | 4.20E+04 | 503 |
| Tubulin alpha-1A chain | P68369 | 50 | 4.9 | 51 | 5.3 | 6 | 18 | 1.16E+04 | 1160 |
| | | | | 18 | 5.6 | 5 | 16 | 2.50E+03 | 999 |
| | | | | 56 | 6.0 | 5 | 14 | 1.43E+03 | 444 |

| | | | | | | | | | |
|---|---|---|---|---|---|---|---|---|---|
| | | | | 50 | 5.5 | 10 | 24 | 9.74E+04 | 1161 |
| | | | | 49 | 5.5 | 8 | 32 | 7.95E+04 | 494 |
| | | | | 42 | 6.8 | 8 | 27 | 3.15E+05 | 700 |
| Tubulin beta-5 chain | P99024 | 50 | 4.8 | 25 | 5.5 | 9 | 26 | 3.91E+04 | 889 |
| | | | | 47 | 5.4 | 8 | 34 | 1.18E+05 | 649 |
| WD repeat-containing protein 61 | Q9ERF3 | 34 | 5.1 | 40 | 4.4 | 12 | 40 | 74[a] | 709 |

Note: The theoretical and experimental molecular mass and p*I* are listed for all the differential spot proteins. The number of peptides that allowed the identification and the corresponding percentage of the sequence covered are also indicated.

[a]Mascot score.

Table S1B Identification of proteins by MALDI-TOF MS in the two-dimensional gels of SAMR1 and SAMP8 astrocytes

| **Protein identified** | **Swiss-Prot Acc. No.** | **Theoretical** | | **Experimental** | | **Match Pept.** No. | **Seq cover** % | **MOWSE score** | **Spot** |
|---|---|---|---|---|---|---|---|---|---|
| | | **Mr** KDa | **p*I*** | **Mr** KDa | **p*I*** | | | | |
| Adenylate kinase isoenzyme 4 | Q9WUR9 | 25 | 7.0 | 37 | 6.7 | 5 | 27 | 7.49E+03 | 671 |
| Acyl-coenzyme A thioesterase 2 | Q9QYR9 | 50 | 6.9 | 69 | 6.7 | 7 | 16 | 1.27E+03 | 273 |
| Cytochrome c oxidase subunit 4 isoform 1 | P19783 | 20 | 9.3 | 15 | 8.9 | 9 | 52 | 2.23E+05 | 970 |
| Dihydropteridine reductase | Q8BVI4 | 26 | 7. 7 | 39 | 8.5 | 6 | 27 | 2.04E+03 | 634 |
| S-methyl-5'-thioadenosine phosphorylase | Q9CQ65 | 31 | 6.7 | 40 | 7.0 [a]<br>7.3 | 12<br>11 | 51<br>52 | 2.29E+06<br>3.20E+06 | 604<br>1088 |
| Protein-arginine deiminase type-2 | Q08642 | 76 | 5.4 | 50 | 6.7 | 7 | 19 | 3.03E+03 | 412 |
| Poly(rC)-binding protein 1 | P60335 | 37 | 6.7 | 55 | 6.8 | 8 | 36 | 7.30E+05 | 336 |
| Sodium/hydrogen exchanger 5 | Q9Z0X2 | 99 | 6.9 | 53 | 9.4 | 9 | 13 | 2.63E+04 | 364 |
| Aldehyde dehydrogenase | P47738 | 57 | 7.5 | 43 | 6.6 | 7 | 22 | 2.23E+04 | 597 |
| Stomatin-like protein 2 | Q99JB2 | 38 | 9.0 | 53 | 6.4 | 6 | 24 | 1.01E+04 | 361 |
| Myosin light polypeptide 6 | Q60605 | 17 | 4.6 | 15 | 3.9 | 4 | 36 | 1.61E+02 | 903 |
| Macrophage-capping protein | P24452 | 39 | 6.7 | 58 | 7.1 | 6 | 32 | 1.27E+04 | 1075 |
| Actin, cytoplasmic 2 | P63260 | 42 | 5.3 | 15 | 6.8 | 7 | 28 | 6.06E+03 | 969 |
| Coatomer subunit epsilon | O89079 | 35 | 4.9 | 51 | 4.8 | 11 | 43 | 7.70E+06 | 500 |

Note: The theoretical and experimental molecular mass and p*I* are listed for all the differential spot proteins. The number of peptides that allowed the identification and the corresponding percentage of the sequence covered are also indicated.

[a]First data for SAMR1 and second for SAMP8 for the all row.

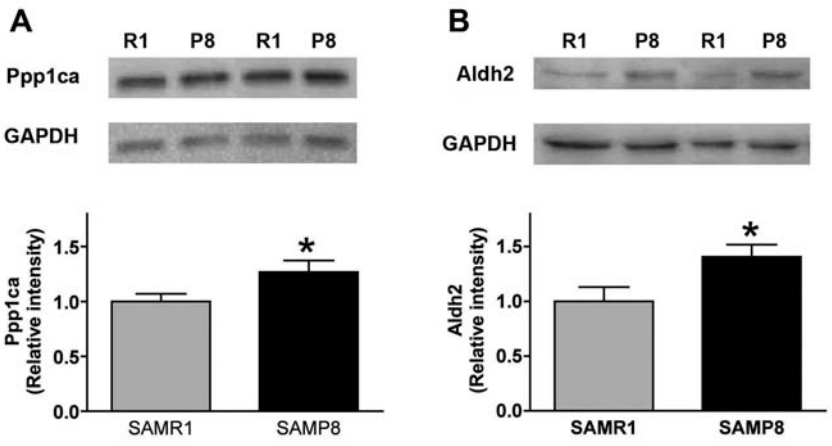
A
R1
P8
R1
P8
Ppp1ca
GAPDH
Ppp1ca
(Relative intensity)
1.5
1.0
0.5
0.0
*
SAMR1
SAMP8
B
R1
P8
R1
P8
Aldh2
GAPDH
Aldh2
(Relative intensity)
1.5
1.0
0.5
0.0
*
SAMR1
SAMP8